Dynamic Constitutive Model for Polymers with Considering Strength-Differential Effect and Strain Rate Dependency

T.Tsuda[1], A.Abe[2], R.Akita[2], T.Numata[3], K.Mimura[4], S.Tanimura[5]
[1]*ITOCHU Techno-Solutions Corporation, Umeda, Kita-ku, Osaka, Japan*
[2]*ITOCHU Techno-Solutions Corporation, Kasumigaseki, Chiyoda-ku, Tokyo, Japan*
[3]*Sumitomo Bakelite Co., Ltd., Murotani, Nishi-ku, Kobe, Japan*
[4]*Osaka Prefecture University, Gakuen-cho, Naka-ku, Sakai, Japan*
[5]*Emeritus Professor of Osaka Prefecture University and of Aichi University of Technology*

Abstract

It is known that the dynamic behavior of polymers depends greatly on not only the strain rate but also the hydrostatic pressure, and furthermore, the volumetric change after plastic deformation is larger than that of the metal material. Therefore, it is necessary to clarify these material properties for high precision simulation of polymers.
In this study, we newly extended the Tanimura-Mimura 2009 model to simulate the dynamic behavior of polymers which depends not only on the strain rates but also on the hydrostatic pressure, and implemented using the user subroutine function of the impact analysis code LS-DYNA®. Then, dynamic tension and compression tests were performed on polycarbonate specimens using the Sensing Block Type High Speed Material Testing System, and material parameters of the extended constitutive equation were determined. Furthermore, verification simulation by LS-DYNA using these constituent equation and material parameters was carried out. As a result, the simulation of the dynamic behavior of tension and compression agreed well with the dynamic test results, and the validity of the constitutive equation and its material parameters were confirmed.

1. Background

In recent years, the use of polymeric materials as a strength member of vehicles is extending steadily. Dynamic properties of a variety of metals and plastics were studied using the Sensing Block Type High Speed Material Testing System (SBTS, SAGINOMIYA SEISAKUSHO, INC.), covering a wide range of strain rates and a large strain region up to the true failure strain, and the values of parameters for the Tanimura-Mimura 2009 model (T-M 2009 model) had been obtained [1], [2], [3]. Applicability of the commonly used rate-dependent constitutive models were discussed comparing the properties of these models with experimental data [4]. It is clearly shown by the comparison that the T-M 2009 model is especially useful for large deformations up to failure. It is known, however, that the dynamic behavior of polymers depends not only on the strain rates but also on the hydrostatic pressure, and exhibits the SD effect (Strength-Differential effect) with different tensile and compressive yield stresses. Furthermore, unlike metals, the volumetric change due to craze during plastic deformation cannot be ignored for polymeric materials, and these material properties also need to be clarified for high-precision simulation of polymers. In numeric simulation, there are not any high-precision and convenient constitutive models for polymers. LS-DYNA has an excellent constitutive model SAMP-1 [5] developed for polymers, but it has been pointed out that it is necessary to set a lot of input parameters and takes time to calculate.

In this study, we extend the T-M 2009 model to simulate the dynamic behavior of polymers which depends not only on the strain rates but also on the hydrostatic pressure, and exhibits the SD effect. Then, it was implemented into LS-DYNA as a user defined constitutive model.

Next, tension and compression experiment for a polycarbonate was carried out using the SBTS, and the values of the material parameters of the extended constitutive model were obtained. Furthermore, verification

simulation by LS-DYNA using the constitutive model and its material parameters was carried out. As a result, the dynamic behavior of tension and compression by simulation agreed well with the dynamic test result, the validity of the extended constitutive model and material parameters was confirmed.

2. Constitutive model for polymers

2.1 Yield function

We adopted the hydrostatic pressure dependency yield function proposed by Sanomura [6] as a yield function with considering the SD effect between tension and compression in a uniaxial loading.
The Sanomura's yield function is expressed by

$$f = \bar{\sigma} - \sigma_y = (1-\xi)\sqrt{3J_2} + \xi I_1 - \sigma_y = 0, \quad (1)$$

where, J_2 and I_1 represent the second invariant of the deviatoric stress S_{ij} and the first invariant of the stress σ_{ij}, respectively ($J_2 = \frac{1}{2}S_{ij}S_{ij},\ I_1 = \sigma_{ii}$), $\bar{\sigma}$ represents the equivalent stress, σ_y represents the yield stress at uniaxial tension and ξ represents material parameter. This yield function shows a linear relationship to hydrostatic pressure as shown in Figure 1. The σ_y in the Figure is the yield stress in a uniaxial tension.

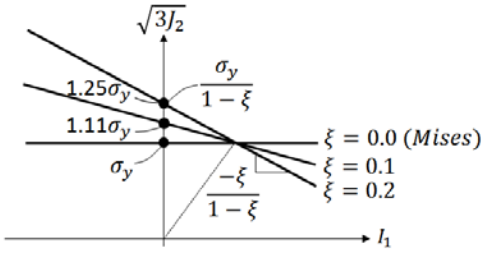

Figure 1 Hydrostatic pressure dependent yield function

The parameter ξ represents the magnitude of the SD effect and depends on equivalent plastic strain $\bar{\varepsilon}^p$, and is expressed by

$$\xi(\bar{\varepsilon}^p) = \frac{{\sigma_y}^c - {\sigma_y}^t}{2{\sigma_y}^c}, \quad (2)$$

where, ${\sigma_y}^c$ and ${\sigma_y}^t$ represent the flow stress at compression and tension in a uniaxial loading, respectively as shown in Figure 2. Here, we call this the SD effect parameter. The value of ξ takes a value from 0 to 1 ($0 \le \xi < 1$) and if $\xi = 0$ the yield function shown in equation (1) matches the Mises yield function ($f = \sqrt{3J_2} - \sigma_y$).

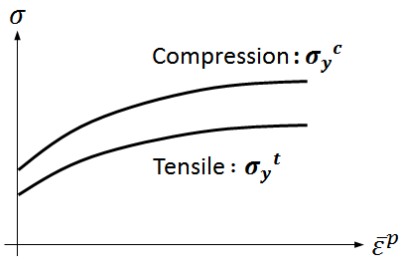

Figure 2 Stress-strain curve at tension and compression

2.2 Flow rule

In order to consider the volumetric change after plastic deformation of polymers, in this study, we assume a non-associated flow rule as shown in equation (3) including hydrostatic stress in plastic potential g [5].

$$g = \sqrt{3J_2 + \zeta p^2} \tag{3}$$

Where, p represents a hydrostatic pressure, ζ represents a parameter representing the dependence of pressure in the plastic potential, and has a relationship shown in equation (4) with plastic Poisson's ratio ν_p. Here, if $\nu_p = 0.5$, then ζ becomes zero, the flow rule shown in equation (3) matches with the equation of Prandtl-Reuss.

$$\zeta = \frac{9}{2}\frac{1-2\nu_p}{1+\nu_p}, \tag{4}$$

2.3 Strain rate effect

The T-M2009 model [1] developed by Tanimura et al. is as shown in equation (5).

$$\sigma = \sigma_s + \left\{\alpha \cdot (\varepsilon_p)^{m1} + \beta\right\} \cdot \left(1 - \frac{\sigma_s}{\sigma_{CR}}\right) \cdot ln\left(\frac{\dot{\varepsilon}_p}{\dot{\varepsilon}_{sp}}\right) + B(\varepsilon_p, \sigma_s) \cdot \left(\frac{\dot{\varepsilon}_p}{\dot{\varepsilon}_u}\right)^{m2} \tag{5}$$

The first term in the right side of the equation (5) represents the quasi-static stress, the second the incremental flow stress depends on the strain rate, and the third the dramatic increase of stress at a high strain rate range for metal, but it is negligible since its effect is hardly observed in polymers. Where σ is the flow stress, σ_s is the stress at a lower plastic strain rate $\dot{\varepsilon}_{sp}$, ε_p is the equivalent plastic strain, $\dot{\varepsilon}_p$ is the equivalent plastic strain rate, $\dot{\varepsilon}_{sp}$ is the lower limit value of strain rate range and chosen as 10^{-2} [1/sec] for the tested material group, $\dot{\varepsilon}_u$ is the unit of strain rate [=1/sec], σ_{CR} is the critical stress under uniaxial tension or compression, $\alpha, \beta, m1, m2$ are material parameters specified for each material group. Note it is assumed originally that the strain rate dependence of the flow stress in polymers is isotropic and it does not depend on the hydrostatic pressure. We now consider the first term in equation (5) to be $(1-\xi)\sqrt{3J_2} + \xi I_1$ as shown in equation (1).

2.4 Stress integration method

Stress integration was done by implicit method, and the radial return algorithm was applied to the deviation stress component and the pressure component, respectively.

2.5 Input card format

The input card format in our constitutive model is shown below.

*MAT_USER_DEFINED_MATERIALS

Card 1

Variable	MID	RO	MT	LMC	NHV		IBULK	IG
Default	none	none	41	32	4		4	5

Card 2

Variable	IVECT	IFAIL	ITHERM	IHYPER	IEOS			
Default	0	0	0	0	0			

Card 3

Variable	MTYP	E	NU	K	G			LCIDT
Default	0	none	none	none	none			none

Card 4

Variable	NUNITM	NUNITL	NUNITT	EPSR0	SM	RLIMIT	-	FAIL
Default	4	1	3	0.01	0.1	1.0e+5	-	0.0

Card 5 (For Polymers)

Variable	XI	VUEP						
Default	0.0	0.5						

Card 6 (Additional card for MTYP=0)

Variable	ALPHA	BETA	M1	SCR	M2	B1	B2	
Default	none	none	none	none	none	none	none	

Here, the parameter MTYP on Card 3 is the material group ID of the material database. E is the Young's modulus, NU is the Poisson's ratio. LCIDT is the load curve ID defining effective stress versus effective plastic strain in tension at quasi-static. The parameter FAIL on Card 4 is failure flag. If FAIL>0.0, FAIL is plastic strain to failure. If FAIL=0.0, failure is not considered. If FAIL<0.0, |FAIL| is the load curve ID defining equivalent plastic strain to failure versus triaxiality. The parameter XI on Card 5 is the SD effect flag. If XI>0.0, XI is the SD effect parameter ξ. If XI=0.0, SD effect is not considered. If XI<0.0, |XI| is the load curve ID defining SD effect parameter versus equivalent plastic strain. VUEP is plastic Poisson's ratio flag. If VUEP>0.0, VUEP is constant plastic Poisson's ratio ν_p. If VUEP=0.0, the volumetric change after plastic deformation is not considered. If VUEP<0.0, |VUEP| is the load curve ID defining plastic Poisson's ratio versus equivalent plastic strain. The parameter ALPHA, BETA, M1, SCR on Card 6 are strain rate effect parameter $\alpha, \beta, m1$ and σ_{CR}, respectively. If MTYP=0, the values of material DB are set in them.

3. Material testing and data processing

3.1 Dynamic property test

Dynamic testing of tension and compression on a polycarbonate (PC) was done using the SBTS owned by Osaka Prefecture University. Figure 3 shows the shape of the test piece (the size for tension test is a plate shape with a gauge-length of 5 mm, a width of 2 mm, a thickness of 2 mm, for compression test, a cylindrical shape with a diameter of 6 mm, a height of 6 mm).

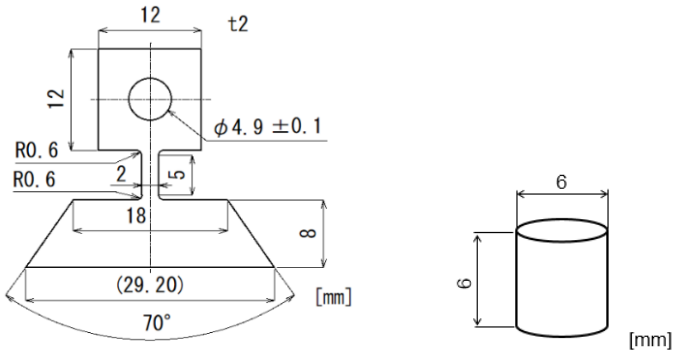

Figure 3 Shape and size of test piece (Left: Tension, Right: Compression)

In the case of the tension test, the test piece is fixed to the test equipment with the upper pin hole and the gauge-length part is pulled by hitting the lower trapezoidal part with the impact block. In the case of the compression test, the test piece is compressed by directly hitting the upper surface of the cylinder with the impact block. At this time, grease was applied to the end face of the compression test piece to reduce the influence of friction.

Dynamic tests were carried out with tensile and compressive strain rates of five levels respectively, and each test was conducted twice under the same conditions and reproducibility was confirmed. Table 1 shows the strain rate in the dynamic test.

Table 1 Strain rate in testing

Testing case	Strain rate in tension [1/sec]	Strain rate in compression [1/sec]
1	0.08	0.083
2	1.2	0.67
3	12	11.7
4	200	66.7
5	700	583.3

Figure 4 and 5 show the shape of test piece in each case after the testing, respectively. This suggests that both tensile and compressive deformation of the parallel part was uniform during the test.

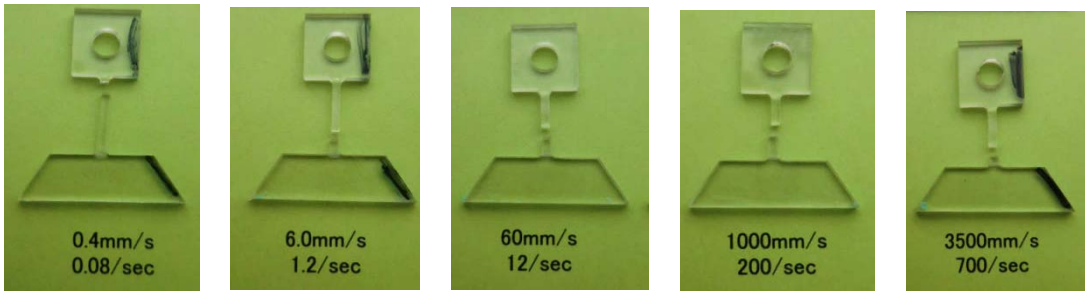

Figure 4 Shape of test piece in each case after tension test

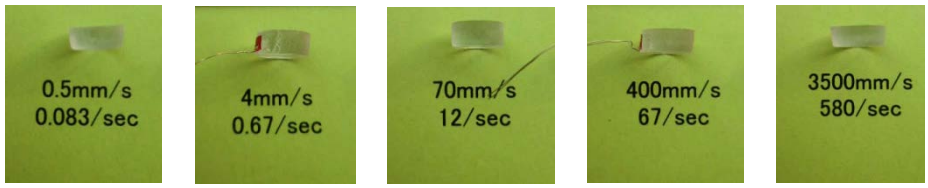

Figure 5 Shape of test piece in each case after compression test

3.2 Data processing

Figure 6 shows the nominal stress-nominal strain relationship for each strain rate level obtained in the dynamic test of tension and compression. Here, the deformation in tension and compression can be regarded as maintaining uniform deformation from the deformed shape after the test shown in Figure 4 and 5. Therefore, it is converted from the nominal value to the true value by the equation (6) and (7) derived from the constant volume condition.

$$\sigma = \sigma_n(1+\varepsilon_n),\ \varepsilon = \ln(1+\varepsilon_n) \qquad \text{at tension} \qquad (6)$$

$$\sigma = \sigma_n(1-\varepsilon_n),\ \varepsilon = -\ln(1-\varepsilon_n) \qquad \text{at compression} \qquad (7)$$

Where, σ is the true stress, σ_n is the nominal stress, ε is the true strain, and ε_n is the nominal strain.

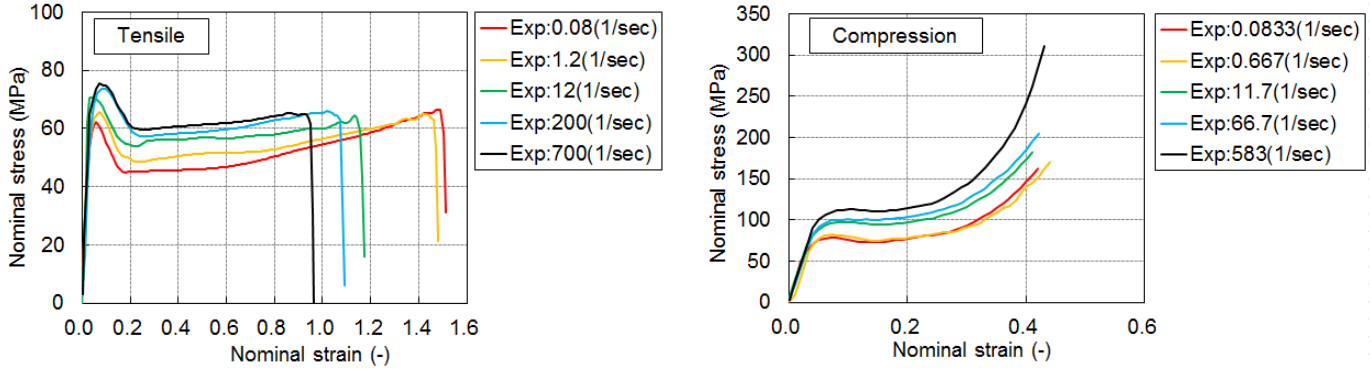

Figure 6 Nominal stress - nominal strain curve (Left: Tension, Right: Compression)

The true stress-true plastic strain relationship obtained by the equation (6) and (7) are shown in Figure 7, respectively. The small square marks in the Figure show a true fracture point calculated by the equation (8) from the cross-sectional area of the test piece at fracture for each strain rate.

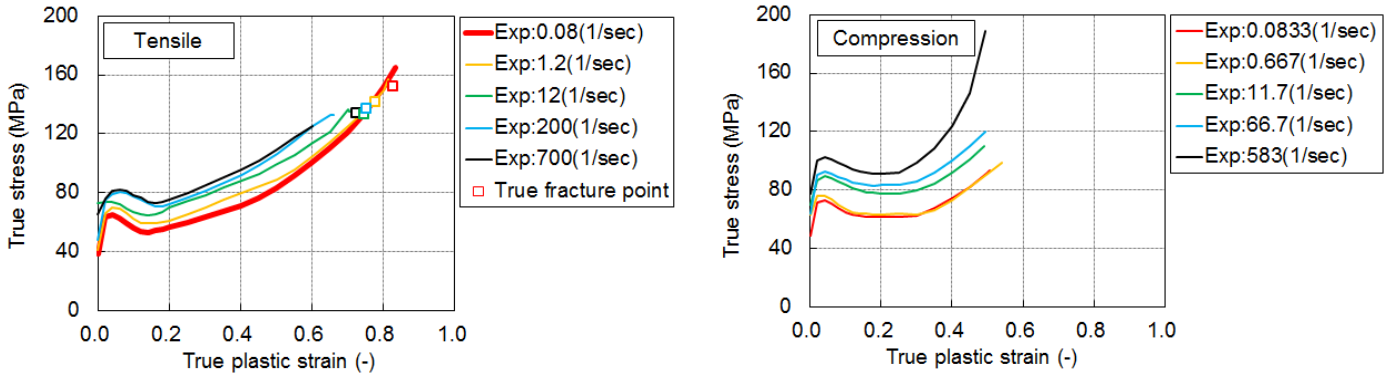

Figure 7 True stress - true plastic strain curve (Left: Tension, Right: Compression)

$$\sigma_f = \sigma_F \left(\frac{A_0}{A_F}\right),\ \varepsilon_f = \ln\left(\frac{A_0}{A_F}\right) \tag{8}$$

Where, σ_F and σ_f are the nominal stress and true stress at fracture, respectively. ε_f is the true strain at fracture, A_0 is the initial cross-sectional area, and A_F is the cross-sectional area of the fracture surface. In measurement of the area of the fracture surface, the influence of elastic return is taken into consideration.

4. Calculation of material parameters

4.1 SD effect parameter

Sanomura obtained $\xi = 0.05$ for the PC in the equation (1) as a constant [5]. However, in this study, it is assumed that ξ is a function of the equivalent plastic strain, and the value of ξ for each plastic strain is calculated by equation (2) from the true stress-true strain relationship of tension and compression shown in the Figure 7. Figure 8 shows the ξ- equivalent plastic strain relationship obtained for each strain rate.

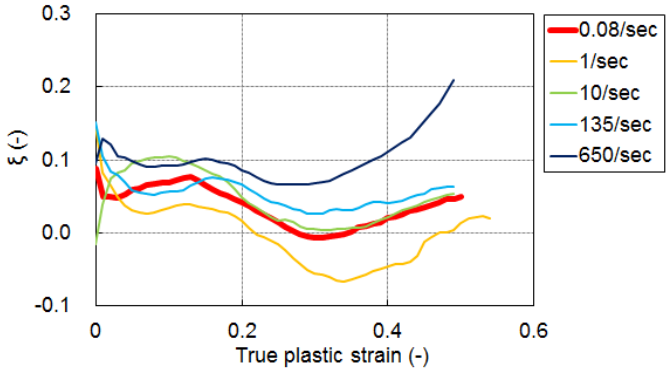

Figure 8 Relationship between ξ- true plastic strain

It is found that the values of ξ vary complicatedly between 0 and 0.1 (except 1 /sec and 650 /sec) with respect to plastic strain, but $\xi = 0.05$ obtained by Sanomura corresponds to this small range as shown in the Figure 8. In this study, it is assumed that the SD effect parameter ξ depends on plastic strain, but does not depend on strain rate. Therefore, the value of ξ obtained from each S-S curve of quasi-static tension and compression are adaptable.

4.2 Strain rate effect parameter

The strain rate dependence of the flow stress for each strain level for the PC is shown in Figure 9. The symbols of solid circle, square, cross, and up triangle etc. in the Figure correspond to the flow stress at each plastic strain for each curve in Figure 8. The dashed straight lines in the Figure are a linear approximation of the symbols for each plastic strain and their tangential coefficient *C* represent the magnitude of the strain rate dependency for the flow stress.

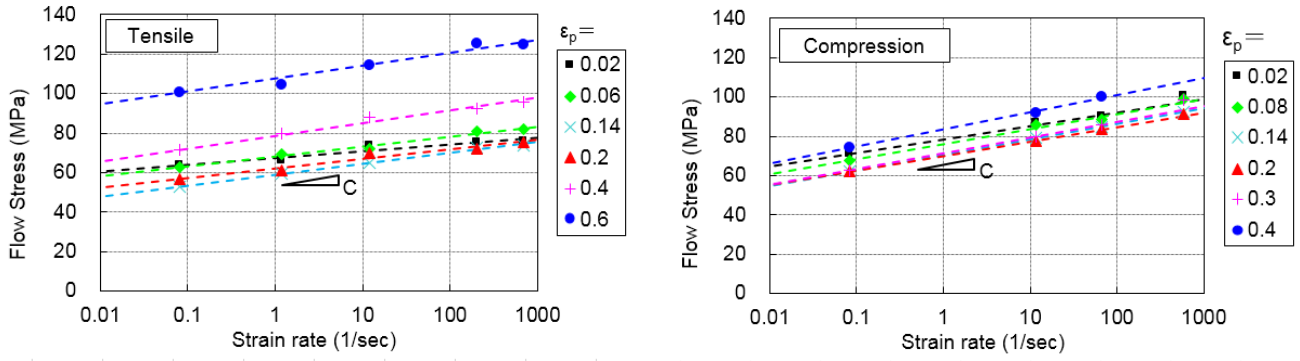

Figure 9 True stress - true plastic strain rate relation for each plastic strain (Left: Tension, Right: Compression)

The normalized strain rate sensitivity gradient $\tilde{C}$ is evaluated from the tangential coefficient *C* in Figure 9, and is expressed by equation (9). In T-M2009 model, this normalized parameter $\tilde{C}$ is summarized as a function of plastic strain and plastic strain rate as shown in equation (10) and the dynamic effect parameters ($\alpha, \beta, m1$ and σ_{CR}) of T-M2009 model can be obtained by approximating the results of equation (9) with equation (10).

$$\tilde{C} = \frac{C}{\sigma_s} = \left(\frac{\sigma}{\sigma_s} - 1\right) / \ln\left(\frac{\dot{\varepsilon}_p}{\dot{\varepsilon}_{sp}}\right) \tag{9}$$

$$\tilde{C} = \left\{\alpha \cdot (\varepsilon_p)^{m1} + \beta\right\} \cdot (1/\sigma_S - 1/\sigma_{CR}) \tag{10}$$

In this study, as we mentioned at the end of chapter 2, it is assumed that the strain rate dependence of flow stress in polymers is isotropic and does not depend on hydrostatic pressure. And, the feature of this extended constitutive model is to approximate the compressive response by applying the SD effect parameter to the tensile S-S curve, and approximate the dynamic response by applying the T-M 2009 parameters to the quasi-static S-S curve. Therefore, we used the dynamic test results of only tension side for identifying the dynamic effect parameters $\alpha, \beta, m1$ and σ_{CR}. The T-M2009 parameters for the PC are shown in "Tension" columns on Table 2. For reference, the parameters obtained from compression results and both results of tension and compression are also shown together.

Table 2 The parameters of T-M2009 model

Material parameter		Tension	Compression	Both
α	[MPa]	3.27	70.8	3.28
β	[MPa]	2.08	4.60	2.43
$m1$	[-]	0.542	4.530	0.420
σ_{CR}	[MPa]	220	220	220

5. Numerical simulation

5.1 Verification calculation

In order to verify our constitutive model shown in Chapter 2 and their material parameters for SD effect and strain rate effect of the PC obtained in Chapter 4, validation analysis was carried out under the same loading conditions as the test using LS-DYNA. Dynamic uniaxial tension and compression analysis were performed with one-element model ($1mm \times 1mm \times 1mm$) as shown in Figure 10. The black mesh line represents the initial geometry, and the red mesh line represents deformed geometry, respectively. The input material property information are shown in Figure 11, 12, 13. In Figure 11, the values surrounded by the red rectangular frame are the main material property values of the PC. Since the measurement test of the volumetric change after the plastic deformation has not yet been carried out, the influence of the volume change is not considered here ($\zeta = 0$). Also, here we does not consider material failure.

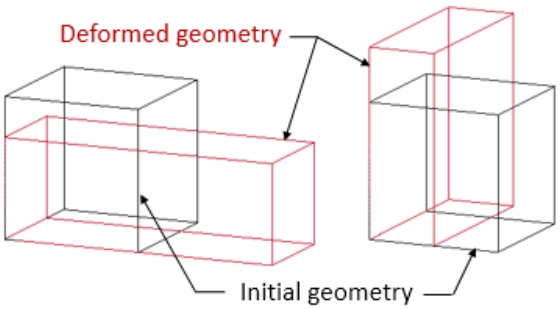

Figure 10 One-element analysis model (Left: Tension, Right: Compression)

```
*MAT_USER_DEFINED_MATERIAL_MODELS
$      MID        RO        MT       LCM       NHV                    IB        IG
         1    1.2e-9        41        32         4                     4         5
$    IVECT     IFAIL    ITHERM    IHYPER      IEOS

$     MTYP         E        NU         K         G                              LCIDT
         0    2250.0      0.35    2500.0     833.3                               10
$   NUNITM    NUNITL    NUNITT     EPSR0        SM    RLIMIT                     FAIL
         4         1         3                                                   0.0
$       XI      NUEP
      -20       0.0
$    ALPHA      BETA        M1       SCR
    3.270      2.08     0.542     220.0
```

Figure 11 Input material property information

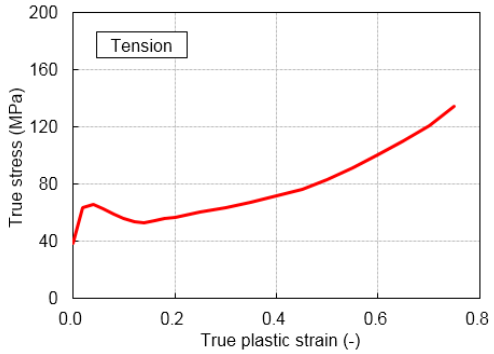

Figure 12 Quasi-static S-S curve of tension (Load curve ID=10)

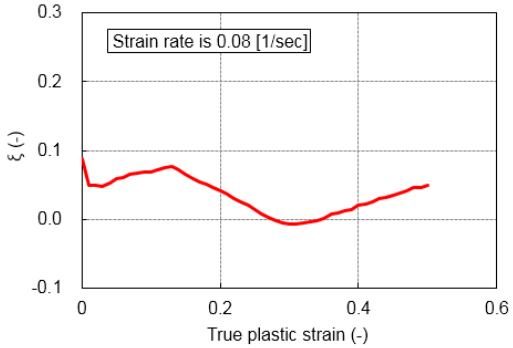

Figure 13 SD effect parameter ξ vs. equivalent plastic strain at strain rate 0.08 [1/sec] (Load curve ID=20)

The simulation results of tension and compression are shown in Figure 14 and 15, respectively, along with experimental results. The solid lines in these Figures are the test results at each strain rate shown in Figure 7 and 8, and the dashed lines are the Mises stress - effective plastic strain relation of the element at each strain rate obtained by the simulation. In the tensile analysis shown in Figure 14, it is found that the simulation result reproduces the experiment well. However, the stress in the medium strain range in high strain rate region is larger than the experiment. The reason for this is considered to be that the influence of the edge effect in the high speed region is increased in the compression test. Especially, in the compression test shown in Figure 15, the stress at strain rate of 583 [1/sec] obviously becomes excessive due to the influence of the edge effect.

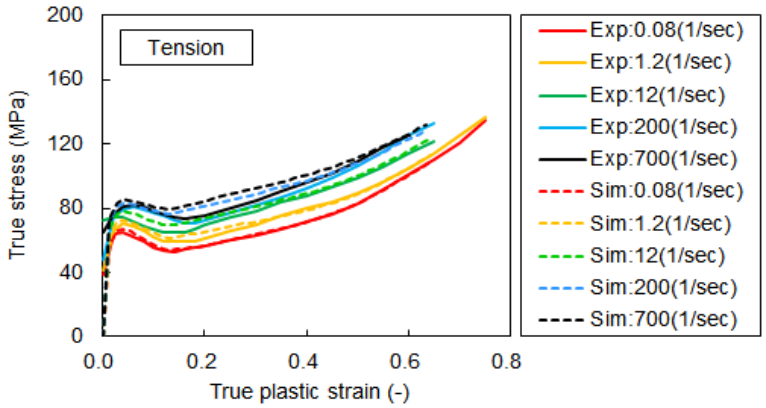

Figure 14 Effective stress - effective plastic strain for tension

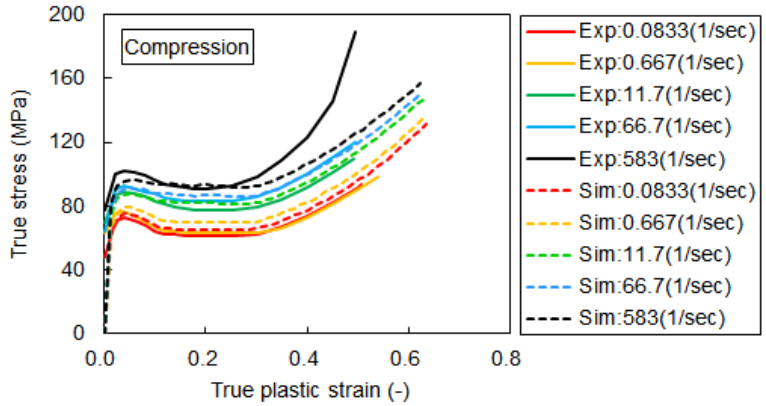

Figure 15 Effective stress - effective plastic strain for compression

5.2 Impact buckling analysis

The impact buckling simulation of a cylinder made of PC with considering the SD effect and the strain rate effect was carried out by the constitutive model for polymers developed in this study and the reaction force versus stroke relation obtained from the simulation was compared with the experimental result. As shown in Figure 16, a weight of 60 kg freely dropped from a height of 0.8 m onto the top surface of the PC cylinder (height: 99.93 mm, out diameter: 32.01 mm, thickness: 2.53 mm). The material properties are shown in Figure 17, 18, 19. Here, note that this PC is another PC different from previous one, so that its material properties shown in the Figure are also different from the previous one. In the Figure 19, the SD effect parameter ξ - effective plastic strain curve was obtained by averaging the curves at each strain rate except the curves at 1 [1/sec] and 650 [1/sec] shown in Figure 8. And, as before, the influence of the volume change is not considered here ($\zeta = 0$).

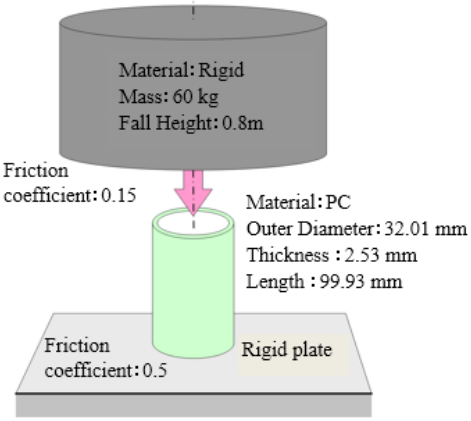

Figure 16 Simulation model

```
*MAT_USER_DEFINED_MATERIAL_MODELS
$ PC-1600
$      MID        RO        MT       LCM       NHV                IB        IG
        41  1.200E-9        41        32         4                 4         5
$    IVECT     IFAIL    ITHERM    IHYPER      IEOS
         1
$     MTYP         E        NU         K         G      ETAN      SIGY      LCID
         0  2.400E+3     0.380    3333.3    869.57                             10
$   NUNITM    NUNITL    NUNITT     EPSR0        SM    RLIMIT                FAIL
         4         1         3                                                0.0
$       XI      NUEP
       -20      0.00
$    ALPHA      BETA        M1       SCR
     0.000      3.00      1.00     220.0
```

Figure 17 Input material property information

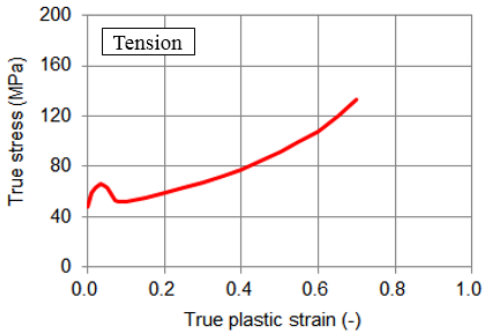

Figure 18 Quasi-static S-S curve for tension (Load curve ID=10)

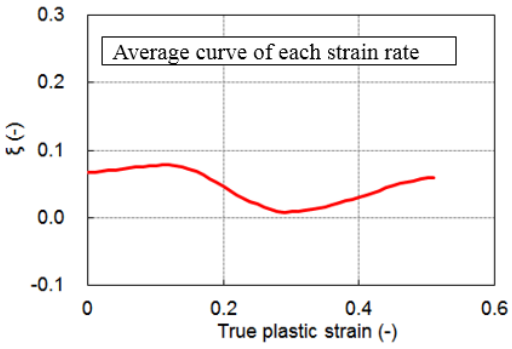

Figure 19 SD effect parameter vs. equivalent plastic strain (Load curve ID=20)

As the analysis result, Figure 20 shows the relationship between the reaction force acting on the weight and the deformation stroke of the PC cylinder together with the experimental results. In the Figure, the dashed line is the result of the experiment, the red solid line and blue solid line are the simulation results with the SD effect and without the SD effect, respectively. The peak reaction force of the simulation with considering the SD effect is good agreement with the experiment. Compression is dominant in buckling phenomenon, so it can be seen that the SD effect should be considered for polymers like PC material. Figure 21 shows the deformed shape after buckling. It is found that diamond buckling with the same mode occurs at the top of the cylinder in both experiment and simulation. However, the deformed height in the simulation is around 10 percent shorter than the experiment. Investigation of this cause is one of our research subjects in the future.

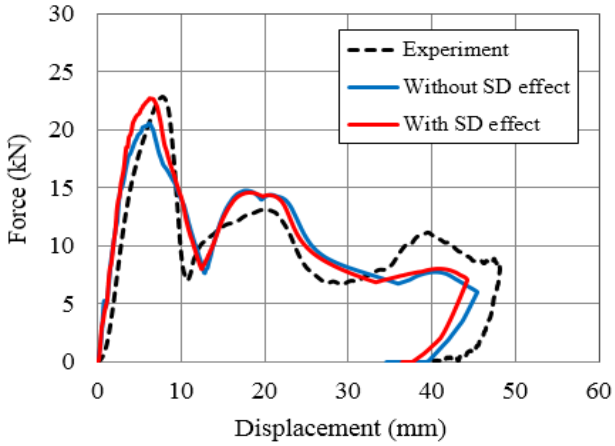

Figure 20 Reaction force - stroke relation

Figure 21 Deformed shape after buckling (Left: Experiment, Right: Simulation)

6. Conclusion

Validation analysis for PC was carried out using our new constitutive model that considers hydrostatic pressure dependence and strain rate dependence. As a result, the same dynamic behavior as the tension and compression test results was reproduced, and the validity of the constitutive model and material parameters was confirmed. From now on, we will measure the volumetric change during the plastic deformation and verify the plastic potential with the influence of the hydrostatic stress. And we are planning a rapture test in order to consider the dependence of stress triaxiality on failure strain for PC. Furthermore, we are planning to obtain the SD effect parameter ξ for not only PC but also other polymers.

References

[1] S. Tanimura, H. Hayashi, T. Yamamoto, K. Mimura, “Dynamic Tensile Properties of Steels and Aluminum Alloys for a Wide Range of Strain Rates and Strain”, Journal of Solid Mechanics and Materials Engineering, Vol.3, No.12, 2009, pp.1263-1273.

[2] T. Tsuda, S. Tanimura, A. Abe, M. Katayama, T. Sakakibara, “Implementation of the Tanimura-Mimura’s Strain Rate Dependent Constitutive Model in LS-DYNA Using User Defined Material Model”, 11th International LS-DYNA Users Conference, 2010, pp.2-47 - 2-58.

[3] T. Tsuda, H. Hayashi, T. Yamamoto, A. Abe, S. Tanimura, “Dynamic Tensile Properties of Engineering Plastics over a Wide Range of Strain Rates”, Journal of Solid Mechanics and Materials Engineering, Vol.6 No.6, 2012, pp.711-720.

[4] S. Tanimura, T. Tsuda, A. Abe, H. Hayashi and N. Jones, “Comparison of rate-dependent constitutive models with experimental data”, International Journal of Impact Engineering, 69, (2014), pp.104-113.

[5] S.Kolling, A. Haufe, M. Feucht, P.A. Du Bois,”A Constitutive Formulation for Polymers Subjected to High Strain Rates”, 9th International LS-DYNA Users Conference, 2006, pp.15-55 - 15-73.

[6] Y. Sanomura, “Constitutive equation for plastic behavior of hydrostatic pressure dependent polymers”, Journal of the Society of Materials Science, Vol.50, No.9, pp968-972 (2001).